Stabilizing two-term clock-drift inversion in ocean bottom node processing

Beng Seong Ong, Zhaojun Liu, and Carsten Udengaard, TGS*

Summary

In marine ocean bottom node (OBN) processing, removing the effects of water velocity variation and correcting for node positions and clock-drifts reduce statics in the data. Clock-drift for ocean-bottom nodes is usually modeled by two terms, a linear and a quadratic term.

A global approach to invert for water velocity, node positions and clock-drift encounters further complication due to the two-term clock-drift. The unstable inversion of clock-drift compromises the quality of inversion for water velocity and node position. To avoid such instability, we illustrate a strategy that helps to minimize the leakage from clock-drift inversion.

Introduction

In OBN processing, removing the effects of water velocity, and correcting for node positions (x, y, z) and clock-drifts removes jitters in the data. Removing such jitters is beneficial in obtaining a quality image. This process becomes even more crucial for 4D processing as correcting the differences in water velocity, node position and clock-drift will improve the 4D signal to noise ratio.

Each receiver node has 5 unknown components, 3 related to node positions and 2 related to clock-drift. The number of water velocity variations can be chosen to be the total number of shots in the whole survey (one unknown per shot) or as the number of shot-lines (one unknown per shot-line) or any other way to partition them, such as by time period (Doherty & Hays 2012). Therefore, the huge number of components that have coupling between them makes it a very challenging inversion problem.

There are a few ways to invert for these components. Some methods opt for inverting in a certain domain for a subset of these components while holding the others fixed, followed by changing the sort order and inverting for the rest of the components that were previously held fixed. This is repeated several times. Such methods are "local" in nature. A global approach inverts for all of these components concurrently. Our work follows the latter approach.

The clock-drift is usually modeled as a linear combination of two terms, which are linear and quadratic (Olofsson & Woje, 2010). In recent acquisition, the total amount of clock-drift within the duration of the survey is available. This information can be used as a constraint.

However, even with this constraint, the inversion could produce linear and quadratic terms of different signs, which are unreasonably large and yet satisfy the constraint. There are also cases where the quadratic term can be larger than the linear term or have opposite signs. Hence introducing fictitious constraints to force the quadratic term to be small or keep them same sign is not fully realistic and will prevent the true solution from being reached in those situations.

Here we present a method to stabilize the inversion to obtain clock-drift within reasonable accuracy using the total drift information as a constraint.

Method

The global inversion approach is based on direct arrival energy as in (Doherty & Hays 2012). We present here the equation used to model the travel-time of direct arrival:

$$\tau_{ij} = \int_{s_i}^{r_j} \frac{dS}{v(z, T_i)} + b_j T_{N,i,j} + a_j \left(T_{i,j}\right)^2 \qquad (1)$$

where

$$T_{i,j} = \left(\frac{T_i - T_j^0}{T_j^f - T_j^0}\right) \in [0,1] \qquad (2)$$

Here τ_{ij} is the direct arrival that follows ray-path from source i (s_i) at time T_i and to receiver j (r_i). T_j^0 and T_j^f are respectively the times when clock is synchronized before and after deployment. The clock-drift terms in (1) are normalized as in (2). The normalization makes it very convenient to describe a total drift constraint. The coefficient of the linear term is b_j, which for simplicity we refer to as linear term for the rest of this paper and the coefficient of quadratic term, a_j as the aging term. The aging term definition is different than what is commonly used (Olofsson & Woje, 2010; Doherty & Hays 2012) but is related.

Let m denote the vector containing the water velocity model change, all shot positions, all receiver positions and coefficients of the clock-drift. Then the global inversion in this case refers to seeking a least-square solution m such that

$$\min_m \left\| FB_{pick} - \tau(m) \right\|^2 \qquad (3)$$

and satisfying constraints of the total drift, d_j:

$$a_j + b_j = d_j \ \ \forall \ receiver\ j \qquad (4)$$

This problem is inherently nonlinear and in order to obtain an accurate solution, we have chosen to deal with nonlinearity instead of solving a linearized version of the least-squares problem. There are many nonlinear algorithms available and we chose the constrained Levenberg-Marquardt (LM) method to tackle this problem. The unconstrained Levenberg-Marquardt algorithm can be found in [Levenberg (1944) and Marquardt (1963)]. In brief, the algorithm a mix of Gauss-Newton and nonlinear gradient descent but more robust than Gauss-Newton and faster convergence rate than nonlinear gradient descent.

We give a brief outline of the Augmented Lagrangian Algorithm (ALA) using LM here (Kochenderfer & Wheeler, 2019). A constrained minimization problem

$$\min_{m} \|f(m)\|^2 \ \text{ subject to } g(m) = 0$$

can be transformed to an augmented Lagrangian version

$$\min_{m} \|f(m)\|^2 + \mu \left\| g(m) + \frac{z}{2\mu} \right\|^2 \tag{5}$$

Start with $z = 0$ and $\mu = 1$ and initial solution m_0.
Loop from $k = 0 \ to\ N \ or\ \|g(m_k)\| < \varepsilon$:

1. Use LM to find a minimizer, m_{k+1} to (5) with starting solution m_k
2. Update multiplier: $z_{k+1} = z_k + 2\mu_k g(m_{k+1})$
3. Penalty parameter update:

$$\mu_{k+1} = \begin{cases} \mu_k & if\ \|g(m_{k+1})\| < 0.25\|g(m_k)\| \\ 2\mu_k & otherwise \end{cases}$$

If we just use the above ALA directly, it's likely that we will obtain linear and aging terms that have opposite signs after the first iteration. This could be a poor starting point for second iteration. As iterations increase, the two terms grow to have large absolute values but with opposite signs that still sum to the total drift. Hence, a better approach is to limit the amount of aging in the early iterations and to remove this restriction later. With this approach, we prevent the aforementioned issue and obtain a better first iteration solution. The LM, being a second-order algorithm, can still recover the aging term that was suppressed in earlier iterations.

In terms of algorithm: we start by using an additional constraint on the aging term to force it to be small in an absolute sense. As the iteration of LM increases, this constraint is weakened gradually. The weakened constraint is carried forward in the next iteration of ALA. In later iterations of LM (and therefore ALA), this additional constraint will be weakened to a negligible level.

We demonstrate that even in cases where the absolute value of the aging term is larger than absolute value of linear term, this strategy is still able to solve for both terms accurately.

Synthetic Example

In this simulation, we have used 523 nodes with a grid of 300 m by 300 m arranged in a staggered manner. Shot spacing is 50 m by 50 m for 60988 shots. Node position errors are randomly generated to be between -2 m to +2 m for horizontal components and -5 m to 5 m for the vertical component. Water velocity changes are between -30 m/s and 30 m/s. The linear drift coefficient is to be +/- 3 ms and that for aging to be +/- 0.1 ms. The Hood function is used as the background water velocity. No source error is introduced and the water bottom is set at 2 km depth. One node is intentionally made to have an aging term of 20 ms and linear term of 0.092 ms. We used data with up to 3 km offsets for inversion.

As we can see in the example below, our approach has managed to invert accurately for all the unknowns including the outlier clock-drift. Figure 1b shows that for the circled node without using the proposed method, the modelled first break deviates from the picked first break by more than 0.2 ms. This can be compared to Figure 1c which has error of less than 0.02 ms.

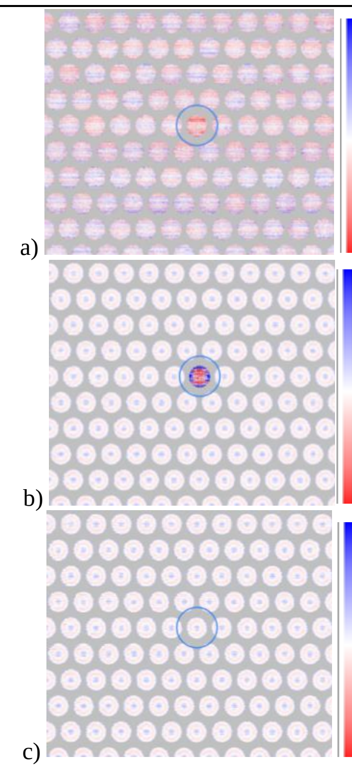

Figure 1: Difference between picked first break and modelled first break; the node circled in blue has an anomalous aging term. a) Initial model. b) Final model without proposed method. c) Final model with proposed method. Scale for a) ranges between -40 ms (red) to 40 ms (blue) and scale for b) and c) ranges between -0.1 ms to 0.1 ms

Stabilizing two-term clock-drift inversion in ocean bottom node processing

Standard Deviation	Linear (μs)	Aging (μs)
W/o proposed method	75	71
Proposed method	11	11

Table 2: Standard Deviation between methods

Figure 3 compares histograms of both linear and aging terms of both methods. Our proposed method has a higher peak and smaller standard deviation (Table 2) for both terms, though both peak locations are about same (-0.04 ms).

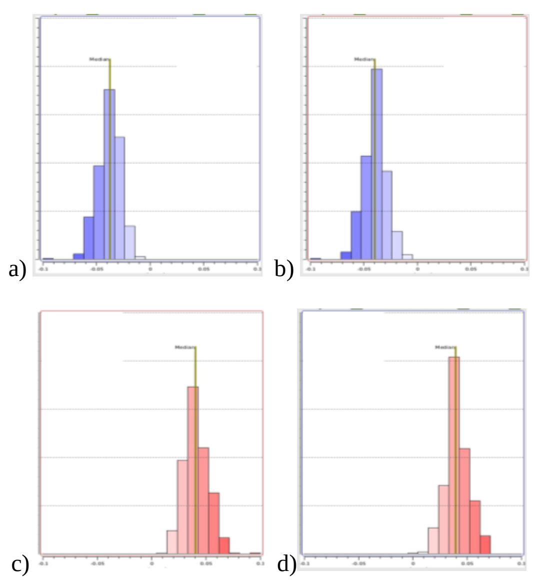

Figure 3: Histograms showing the difference between the inverted and true solutions: (a), (c) without proposed strategy (b), (d) with proposed strategy. (a) and (b) are for the linear term. (c) and (d) are for the aging term. Note that in both linear and aging terms, the proposed solution has a higher peak and smaller deviation. Horizontal axis is from - 0.1 ms to 0.1 ms. Although none are completely centered at zero but the median errors are less than 0.05 ms.Vertical axis is from 0 to 500 thousand.

Field Example

We show a field data example from the Amendment Phase 2 survey which is located in central GoM, across Ewing Bank, Green Canyon, Mississippi Canyon and Atwater Valley. Node spacing is 1200 m with about 2700 nodes that cover 3800 sq-km. Shot spacing is 50 x 100m, dual boat, triple source blended shooting. The water bottom ranges from 200 m to 1400 m. Average maximum offset is about 60 km.

Due to the varying water bottom, we use maximum offset ranging from 500 m to 3 km where we can reliably pick the first break.

We compare here two tests. The first test inverts for node position and water velocity while the second test inverts for the above and clock-drift. We use linear move-out (LMO) as a QC to evaluate the quality of the solution.

Figure 4 shows the LMO QC before and after correction of inverted node positions, water velocity variation and clock-drift. The biggest effect is due to water velocity variation. The clock-drift effect in this example is subtle but is flatter with clock-drift. Figure 5 shows a zoomed in section of Figure 4.

Conclusions

Our method yields stable inversion of clock-drift without jeopardizing inversion stability for node positions and water velocity variation. In the absence of total drift constraints, the same strategy can still be used to obtain reasonable linear and aging terms. Despite using a nonlinear optimization algorithm, there are still small leakages between the different water velocity, node position and clock-drift. Those small leakages could be a result of approximation used in the model.

Acknowledgements

The authors would like to thank TGS for support of this work. We would also like to thank Eric Carmarda and Indranil Samanta for testing and QC.

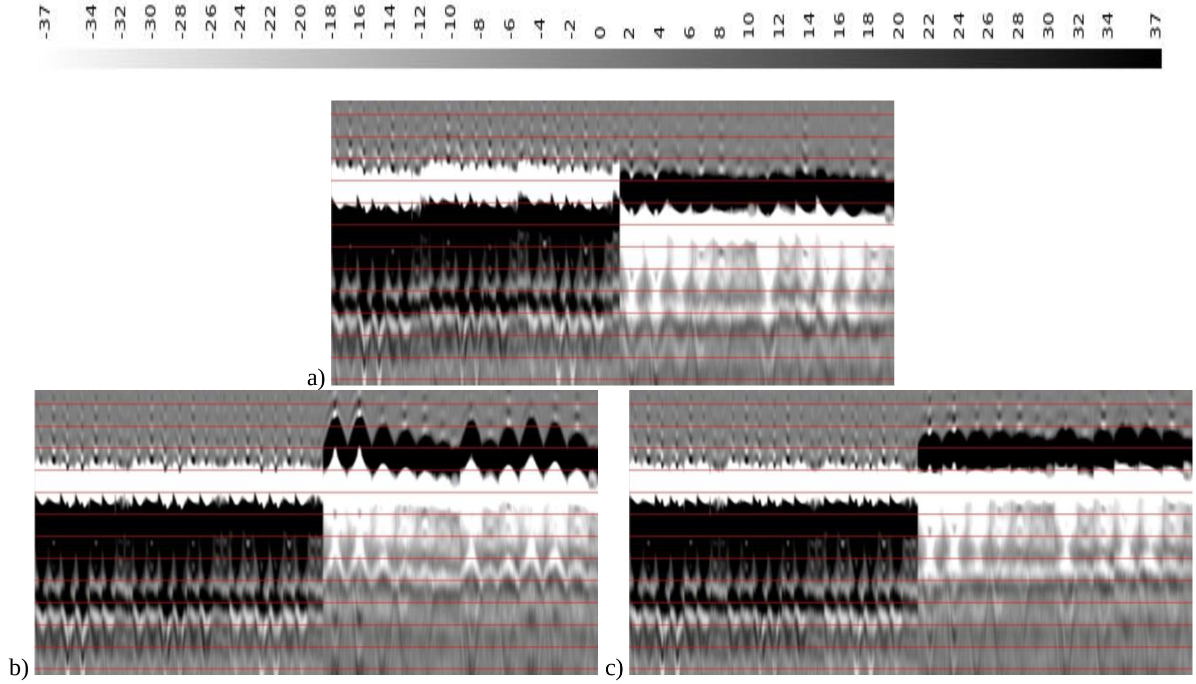

Figure 4: LMO QC of a) Before correction b) After correction for node position and water velocity variation but no clock-drift c) After correction including clock-drift using proposed method. The effect of the clock-drift is small here compared to that of the velocity for th node on the left but more noticable with naked eyes for the node on the right.

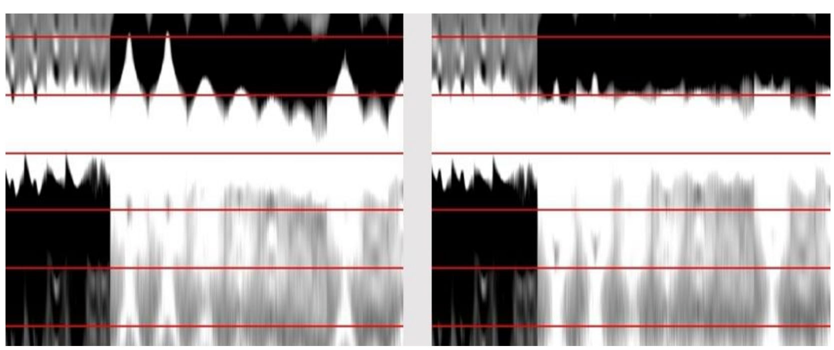

a) b)

Figure 5: Zoomed in section of of Figures 4b and 4c for middle gathers. a) Without clock-drift b) With clock-drift